Journal of Enzyme Inhibition and Medicinal Chemistry, 2010; 25(2): 272–281

informa
healthcare

RESEARCH ARTICLE

Potent inhibitory effects of benzyl and *p*-xylidine-bis dithiocarbamate sodium salts on activities of mushroom tyrosinase

E. Amin[1], A. A. Saboury[1], H. Mansuri-Torshizi[2], and A. A. Moosavi-Movahedi[1]

[1]*Institute of Biochemistry and Biophysics, University of Tehran, Tehran, Iran and* [2]*Department of Chemistry, University of Sistan and Bluchestan, Zahedan, Iran*

Abstract

A novel monofunctional benzyldithiocarbamate, $C_6H_5CH_2NHCSSNa$ (**I**), and a bifunctional *p*-xylidine-bis(dithiocarbamate), $NaSSCNHCH_2C_6H_4CH_2NHCSSNa$ (**II**), as sodium salts, were synthesized by reaction between *p*-xylylenediamine or benzylamine with CS_2 in the presence of NaOH. They were characterized by spectroscopic techniques such as ^1H NMR, IR, and elemental analysis. These water-soluble compounds were examined for their inhibition of both activities of mushroom tyrosinase (MT) from a commercial source of *Agricus bisporus*. L-3,4- Dihydroxyphenylalanine (L-DOPA) and L-tyrosine were used as natural substrates for the catecholase and cresolase enzyme reactions, respectively. Kinetic studies showed noncompetitive inhibition of **I** and mixed type inhibition of **II** on both activities of MT. The inhibition constant (K_I) of **II** was smaller than that of **I**. Raising the temperature from 27 to 37°C caused a decrease in K_I values of **I** and an increase in values of **II**. The binding process for inhibition of **I** was only entropy driven, which means that the predominant interaction in the active site of the enzyme is hydrophobic; meanwhile, the electrostatic interaction can be important for the inhibition of **II** due to the enthalpy driven binding process. Fluorescence studies showed a decrease of emission intensity without a shift of emission maximum in the presence of different concentrations of compounds. An extrinsic fluorescence study did not show any considerable change of the tertiary structure of MT. Probably, the conformation of inhibitor-bound MT is stable and inflexible compared with uninhibited MT.

Keywords: *Mushroom tyrosinase; benzyldithiocarbamate;* p-*xylidine-bis(dithiocarbamate); noncompetitive inhibition; mixed inhibition; inhibition constant*

Introduction

Tyrosinase (monophenol monooxygenase; polyphenol oxidase; E.C. 1.14.18.1) is a copper-containing protein, present in animals, plants, fungi, and microorganisms, which catalyzes the oxidation of monophenols to diphenols (cresolase or monophenolase activity) and/or the oxidation of *o*-diphenols further to reactive *o*-quinones in the presence of oxygen (catecholase or diphenolase activity)[1–7]. Quinones are highly reactive compounds and can polymerize spontaneously to form high-molecular-weight compounds[8]. Tyrosinases are responsible for many biologically essential functions, such as pigmentation, sclerotization, primary immune response, and host defense[9–11]. Tyrosinase plays an important role in the wound healing, melanogenesis, parasite encapsulation, and defensive functions of insects[12–14]. In addition, defects in tyrosinase may cause some diseases such as albinism and vitiligo[15,16].

Tyrosinase from *A. bisporus* was reported to be a hetero tetramer comprising two heavy (H) and light (L) chains with a molecular mass of 120 kDa[17]. The enzyme tyrosinase has three domains, of which the central domain contains two Cu binding sites, called CuA and CuB. For the binuclear copper site in tyrosinase no electron paramagnetic resonance (EPR) signal has been detected, that is, they are strongly anti-ferromagnetically coupled. Each atom of the binuclear copper cluster is ligated to three histidine residues[18]. This pair of copper ions in the active site of the enzyme tyrosinase interacts with both molecular oxygen and its phenolic substrate[17]. Active sites of tyrosinase

Address for Correspondence: A. A. Saboury, Institute of Biochemistry and Biophysics, University of Tehran, Tehran, Iran. Tel: +98-21-66956984. Fax: +98-21-66404680. E-mail: saboury@ut.ac.ir

(Received 12 January 2009; revised 13 May 2009; accepted 01 June 2009)

ISSN 1475-6366 print/ISSN 1475-6374 online © 2010 Informa UK Ltd
DOI: 10.3109/14756360903179351

have three different states of binuclear copper structure (Figure 1): met-tyrosinase (E_{met}), deoxy-tyrosinase (E_{deoxy}), and oxy-tyrosinase (E_{oxy})[19]. Both oxy-tyrosinase and met-tyrosinase can act in catecholase activity while only oxy-tyrosinase is able to catalyze monophenols to *o*-diphenols, and binding of monophenol to met-tyrosinase will inactivate tyrosinase[20].

Browning after harvest is a common phenomenon in crops such as mushrooms, which decreases the commercial value of the product. Loss of whiteness upon storage is a major issue in the mushroom industry. In addition, it is very important in the quality control and economic value of fruits and vegetables[21,22]. Because of the undesirable effects of enzymatic browning, tyrosinase inhibitors should have a range of applications and, hence, a considerable number are known[23]. In addition, standard topical treatments for hyperpigmentation disorders such as melasma and post-inflammatory hyperpigmentation include bleaching with hydroquinone, anti-inflammatory therapy using retinoids, and use of tyrosinase inhibitors. Furthermore, tyrosinase inhibitors may be clinically used for the treatment of some skin disorders associated with melanin hyperpigmentation and are important in cosmetics for skin-whitening effects, so there is a need to identify the compounds that inhibit tyrosinase activity[23–26]. There are a number of tyrosinase inhibitors from both natural and synthetic sources that inhibit monophenolase and diphenolase activities[27–30]. Plant polyphenols, usually referred to as a diverse group of compounds containing multiple phenolic functionalities, have been considered as tyrosinase inhibitors. Flavonoids, one of the most numerous and best-studied groups of plant polyphenols, are widely distributed in the leaves, seeds, bark, and flowers of plants. It was found that flavonoids containing an α-keto group show potent tyrosinase inhibitory activity[31]. This inhibition ability may be explained in terms of the similarity between the dihydroxyphenyl group in L-DOPA and the α-keto group in flavonoids. Kaempferol, quercetin, and the 4-substituted resorcinol skeleton show potent tyrosinase inhibitory activity. However, the effective topical concentration of these compounds in disorders of hyperpigmentation is not yet known. A large number of aldehydes from higher plants such as cinnamaldehyde, anisaldehyde, cuminaldehyde, and cumic acid are characterized as tyrosinase inhibitors[32–36]. Synthetic tyrosinase inhibitors may be used as drugs and chemicals. In the case of clinical drugs, captopril, an antihypertensive drug, and methimazole act as tyrosinase inhibitors[37,38]. Simple chemical species capable of binding to copper, such as cyanide, azide, and halide ions, as expected behave as purely competitive inhibitors toward dioxygen binding, although strong differences have been seen among polyphenoloxidases from different sources[39]. Thiol compounds such as cysteine, *N*-aryl *S*-alkylthiocarbamate derivatives, methimazole, diethyldithiocarbamate, and 2-mercaptobenzothiazole have also been used as inhibitors of tyrosinase from different sources[40–44].

Dithiocarbamates are versatile classes of chelating compounds that have been developed in the last 40–50 years. They are an integral part of industrialized agriculture and medicine, and are used against a broad spectrum of fungi and plant diseases caused by fungi[45]. Dithiocarbamates are used in health care for the management of alcoholism, and have been applied to prevent arthrosclerosis, and for antimicrobial and anti-inflammatory activity and metal transport in membranes[46]. It has been reported that dithiocarbamates can react with HS-containing enzymes and coenzymes of fungal cells, thus blocking their catalytic activity. Enzyme inhibition may also occur by complex formation of the active –CSSNa group with metal atoms of metal-containing enzymes[47]. In recent studies, the inhibitory effects of some *n*-alkyl dithiocarbamates and *n*-alkyl xanthates have been considered[48,49]. In the present investigation, the inhibitory effects of benzyldithiocarbamate and *p*-xylidine-bis(dithiocarbamate) sodium salts are described, as well as kinetic analysis of their action toward both cresolase and catecholase activities at two temperatures of 27 and 37°C.

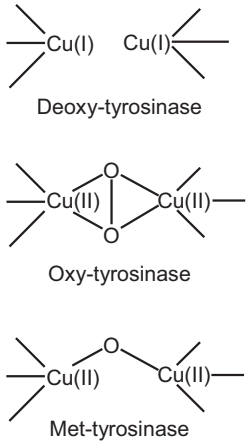

Figure 1. Three different binuclear copper structures in the active site of tyrosinase.

Materials and methods

Materials

Mushroom tyrosinase (MT; E.C. 1.14.18.1; specific activity 5370 units/mg), L-3,4-dihydroxyphenylalanine (L-DOPA), L-tyrosine, and 1-anilinonaphthalene-8-sulfonate (ANS) were purchased from Sigma. Benzyldithiocarbamate

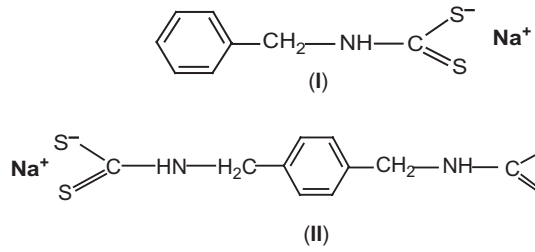

Figure 2. Benzyldithiocarbamate sodium salt (**I**) and *p*-xylidine-bis(dithiocarbamate) sodium salt (**II**).

sodium salt (**I**) and *p*-xylidine-bis(dithiocarbamate) sodium salt (**II**) (Figure 2) were synthesized. Benzylamine, CS_2 and NaOH, (Merck), and *p*-xylylenediamine (Fluka) were used as received. Solvents were of high purity and were used as purchased (Merck), without any further purification. Phosphate buffer (50 mM, pH 6.8) was used throughout this work. All buffers were prepared with water purified by a Milli Q water purification system.

Methods

Melting points were measured on a Unimelt capillary melting point apparatus and are reported uncorrected. Micro chemical analysis of carbon, hydrogen, and nitrogen was carried out on a CHN Rapid Herause analyzer. Infrared (IR) spectra were obtained on a Nicolet 5-DXB FT-IR spectrophotometer in the range 4000–400 cm^{-1} in KBr pellets. ^1H nuclear magnetic resonance (NMR) spectra were recorded on a Bruker DRX-500 Avance spectrophotometer at 500 MHz in DMSO-d_6 using sodium-3-trimethylpropionate as internal reference. ^1H NMR data are expressed in parts per million (ppm) and are reported as chemical shift position (δH), multiplicity (s = singlet, d = doublet, t = triplet, q = quartet, m = multiplet, sb = singlet broad), and assignment.

Synthesis of benzyldithiocarbamate sodium salt, C_6H_5-CH_2-NH-CSSNa (I)

This new ligand was prepared following a method similar to that described earlier[49]. A solution of benzylamine (4.1 mg, 50 mmol) in acetone (40 mL) was treated with NaOH (4 g, 100 mmol) in 40 mL of water. To this solution was added dropwise, with cooling (0°C) and stirring, 10 mL of carbon disulfide. The mixture was stirred in a closed vessel for 2 h with cooling and for 12 h at room temperature, and then the solvent was removed by rotary evaporation at 40°C to complete dryness. The white precipitate left was dissolved in water (40 mL) and filtered. Eighty milliliters of acetone were added, and after one night at 4°C, a white solid was filtered off and washed with acetone and vacuum dried. The yield was 8.20 g, 80%, melting point 71°C. Analysis was calculated for $C_8H_8NS_2Na$: C, 46.83; H, 3.90; N, 6.83; found: C, 46.90; H, 3.92; N, 6.80%. Solid-state IR spectroscopy of the above ligand showed two characteristic bands at 1498 and 931 cm^{-1} assigned to ν (N-CSS) and ν (SCS) modes[50]. ^1H NMR (500 MHz, DMSO-d_6, ppm): 4.67 (d, -CH_2-), 7.25 (m, -C_6H_5-), 8.47 (sb, -NH-).

Synthesis of *p*-xylidine-bis(dithiocarbamate) sodium salt, NaSSC-NH-CH_2-C_6H_4-CH_2-NH-CSSNa (II)

This compound was prepared by following the same procedure as described for (**I**) except that *p*-xylylenediamine was used instead of benzylamine. The yield was 4.11 g, 85%, melting point 297°C. Analysis was calculated for $C_{10}H_{10}N_2S_4Na_2$: C, 36.14; H, 3.01; N, 8.43; found: C, 36.09; H, 2.97; N, 8.02%. Solid-state IR spectroscopy of the above ligand showed two characteristic bands at 1483 and 956 cm^{-1} assigned to ν (N-CSS) and ν (SCS) modes[50]. ^1H NMR (500 MHz, DMSO-d_6, ppm): 4.52 (m, -CH_2-), 7.14 (m, -C_6H_4-), 8.41 (sb, -NH-). Both synthetic compounds dissolved completely in water.

Kinetic measurements

Cresolase and catecholase activities of mushroom tyrosinase were determined by spectrophotometrically measuring the rate of dopachrome formation at 475 nm ($\varepsilon = 3700\ M^{-1}cm^{-1}$) in the first 2 min by using a Cary spectrophotometer, 100 Biomodel, with jacketed cell holders[51]. The assay was performed as previously described with slight modifications[52]. The reaction medium was 1 mL in 50 mM phosphate buffer (pH 6.8). The final concentration of mushroom tyrosinase was 26.07 µg/mL for cresolase activity and 6.52 µg/mL for catecholase activity. Freshly prepared enzyme, substrate, and dithiocarbamates **I** and **II** were used in this work. The reaction was carried out under constant temperatures of 27 and 37°C. Substrate addition followed incubation of the enzyme with different concentrations of synthetic inhibitors. Lineweaver–Burk plots were fitted with weighted linear regression, for qualitative estimation of the type of inhibition. Then, quantitative determination of the K_I values was carried out by nonlinear regression fitting of Michaelis–Menten equations[53–55]. MATLAB Software (version R2008a) was used for regression fitting analysis. Also, the concentration of inhibitor that decreased the rate of enzyme-catalyzed reaction by 50% (IC_{50}) was calculated using the Cornish–Bowden method[56].

Fluorescence studies

Fluorescence intensity measurements were carried out using a Hitachi spectrofluorimeter, MPF-4 model, equipped with a thermostatically controlled cuvette compartment. The intrinsic emission of protein, 0.17 mg/mL, was seen at the excitation wavelength of 280 nm. The extrinsic emission of ANS labeled protein (with 50 concentration ratio) was monitored at the excitation wavelength of 385 nm. The experiments were repeated in the presence of different concentrations of compounds **I** and **II**. All graphs shown were obtained using SigmaPlot.

Results and discussion

The inhibitory effects of two different compounds on both MT activities were examined at pH 6.8 and temperatures of 27 and 37°C.

Kinetic parameters of inhibitory effect of benzyldithiocarbamate sodium salt on activities of MT

When the activities of mushroom tyrosinase at 27°C were assayed using L-DOPA and L-tyrosine as substrates, in catecholase activity the reaction immediately reached a steady-state rate and in cresolase activity the steady-state rate appeared after a lag time (5 s). By the addition of **I**, the initial velocities of reactions were decreased and there was an elongation of lag times (data not shown). To study tyrosinase inhibition by **I** in depth, we observed its effect on the activities of the enzyme, and determined the inhibition

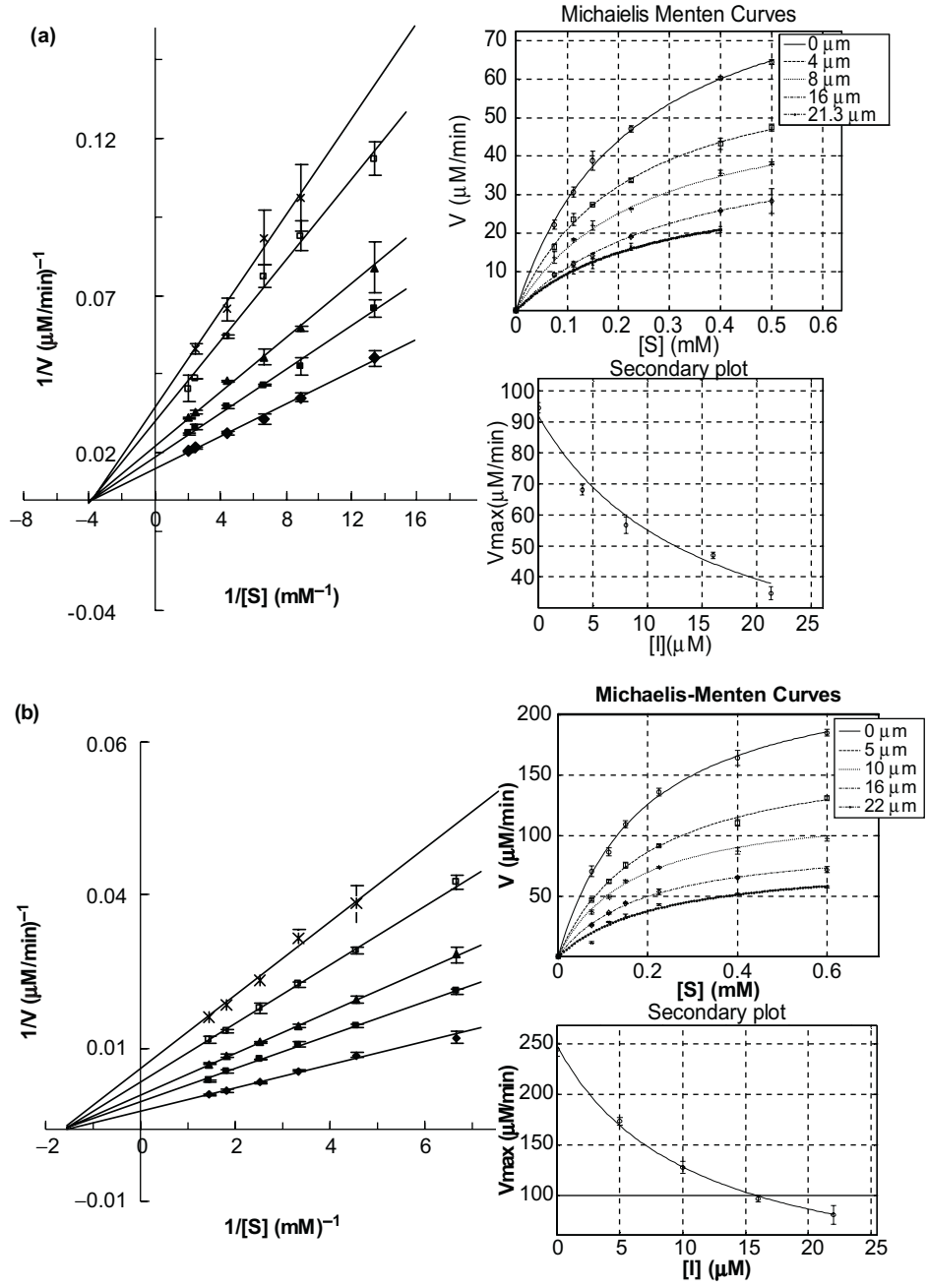

Figure 3. Double reciprocal Lineweaver–Burk plots and nonlinear fittings of mushroom tyrosinase (MT) kinetic assays at temperature of 27°C in the presence of different fixed concentrations of **I** for cresolase reactions (a): 0.0 µM (◆), 4.0 µM (■), 8.0 µM (▲), 16.0 µM (□), 21.3 µM (*), and for catecholase reactions (b): 0.0 µM (◆), 5.0 µM (■), 10.0 µM (▲), 16.0 µM (□), 22.0 µM (*). Insets: secondary plots of fitting V versus [S] and V_{max} versus [I] are shown, [I] is inhibitor.

constant (K_I). To obtain the type of inhibition exerted by **I** on activities of mushroom tyrosinase, the velocity of reaction (V) was measured as a function of the substrate concentration for several concentrations of inhibitor. Double reciprocal Lineweaver–Burk plots in the presence of different concentrations of compound **I** are shown in Figure 3. A series of straight lines in both activities intersect exactly on the horizontal axis. The Michaelis constant (K_m) value was not changed by **I**, but the apparent maximum velocity (V'_{max}) value was decreased, which confirmed the noncompetitive type of inhibition. Then, the values of apparent maximum velocity (V'_{max}) at any concentration of **I** were obtained from nonlinear regression fittings of Michaelis–Menten curves (upper inset). These values were fitted versus inhibitor concentrations (lower inset)[53]. V'_{max} was decreased by a factor $(1+[I]/K_I)$. Nonlinear fitting gave the inhibition constants (K_I) of reaction activity. K_I of cresolase and catecholase activity inhibition was obtained with values of 14.1 µM and 9.4 µM, respectively.

In order to understand the effect of temperature on inhibition and to shed light on the nature of **I** binding with MT, we repeated the above procedure at 37°C (Figure 4, Table 1), and

the change of Gibbs standard free energy of binding ($\Delta G°$) was calculated using the association binding constant (K_a), obtained from the inverse of the K_I value, in Equation (1)[57]:

$$\Delta G° = -RT \ln K_a \tag{1}$$

where R is the gas constant and T is the absolute temperature. Also, calculated K_a values at two temperatures in the van't Hoff equation gives the standard enthalpy change of binding ($\Delta H°$)57:

$$\ln \frac{K_{a2}}{K_{a1}} = -\frac{\Delta H°}{R}\left(\frac{1}{T_2} - \frac{1}{T_1}\right) \tag{2}$$

where K_{a1} and K_{a2} are association binding constants at two temperatures of T_1 and T_2, respectively. Finally, the standard entropy change ($\Delta S°$) was calculated using Equation (3)[57]:

$$\Delta S° = \frac{(\Delta H° - \Delta G°)}{T} \tag{3}$$

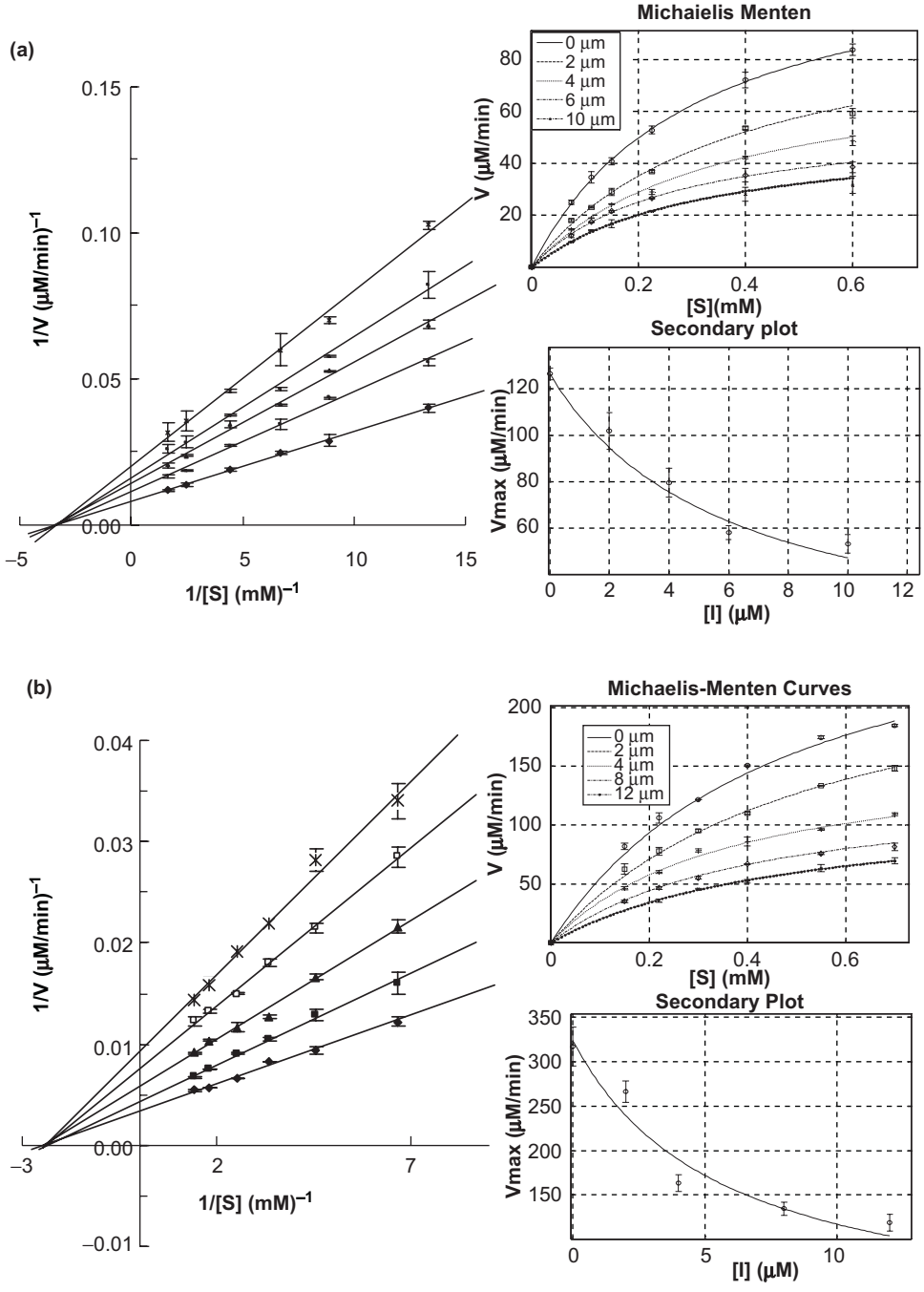

Figure 4. Double reciprocal Lineweaver–Burk plots and nonlinear fittings of MT kinetic assays at temperature of 37°C in the presence of different fixed concentrations of **I** for cresolase reactions (a): 0.0 µM (◆), 2.0 µM (■), 4.0 µM (□), 6.0 µM (▲), 10.0 µM (*), and for catecholase reactions (b): 0.0 µM (◆), 2.0 µM (■), 4.0 µM (□), 8.0 µM (▲), 12.0 µM (*). Insets: fitted V versus [S] and V_{max} versus [I] are shown, [I] is inhibitor.

Table 1. Thermodynamic parameters of binding **I** on mushroom tyrosinase at two different temperatures (±SD).

Reaction type	Temperature (°C)	K_I (μM)	K_a ($M^{-1} \times 10^5$)	$\Delta G°$ (kJ.mol^{-1})	$\Delta H°$ (kJ.mol^{-1})	$T\Delta S°$ (kJ.mol^{-1})
Cresolase	27	14.1±2.1	0.71±0.11	–27.9±0.4	67.4±2.3	95.2±2.7
	37	5.9±0.7	1.69±0.20	–31.0±0.3		98.4±2.6
Catecholase	27	9.4±0.9	1.06±0.10	–28.9±0.2	38.7±9.3	67.5±9.5
	37	5.7±1.6	1.75±0.49	–31.1±0.7		69.8±9.0

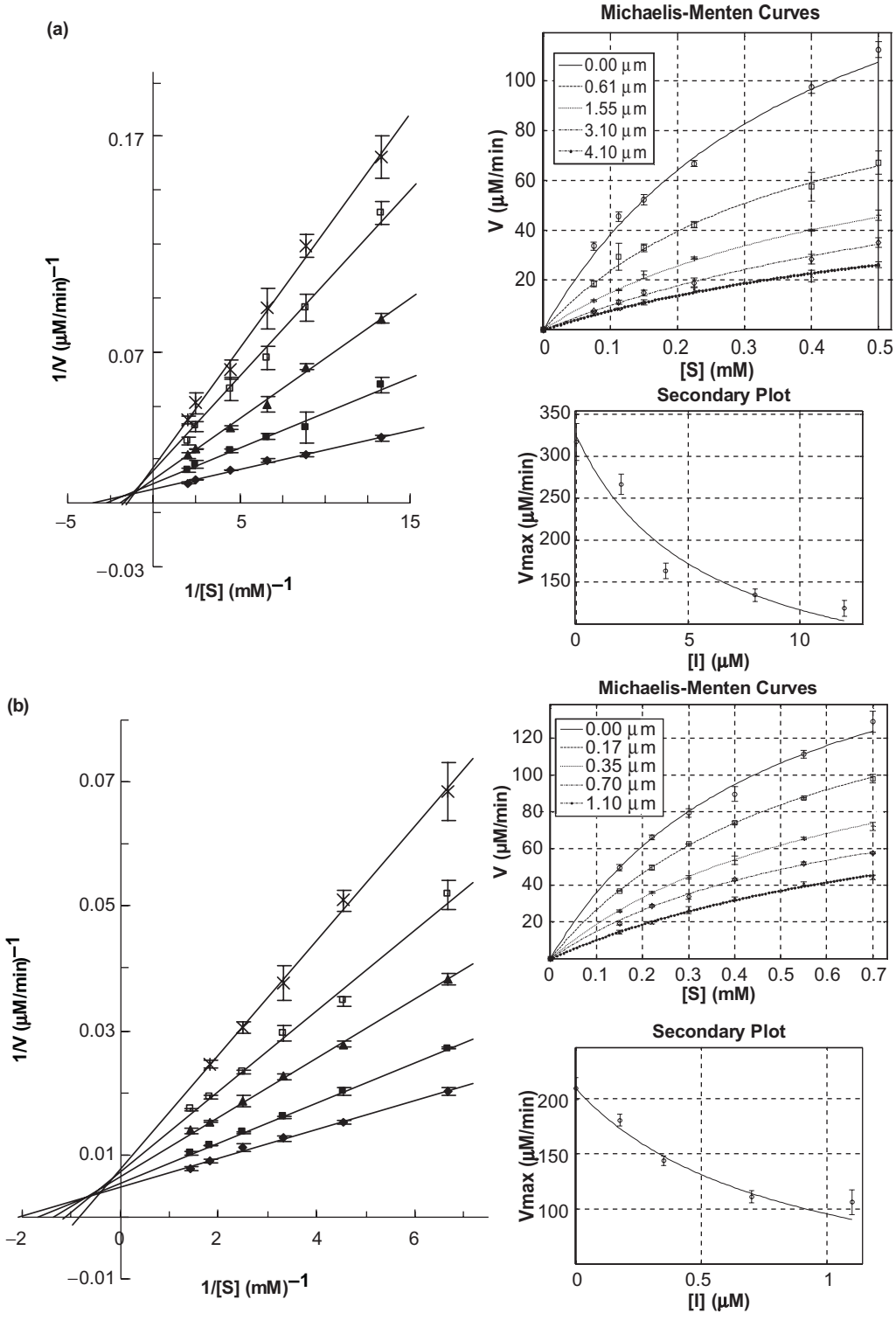

Figure 5. Double reciprocal Lineweaver–Burk plots and nonlinear fittings of MT kinetic assays at temperature of 27°C in the presence of different fixed concentrations of **II** for cresolase reactions (a): 0.0 μM (◆), 0.61 μM (■), 1.55 μM (□), 3.10 μM (▲), 4.10 μM (*), and for catecholase reactions (b): 0.0 μM (◆), 0.17 μM (■), 0.35 μM (□), 0.70 μM (▲), 1.10 μM (*). Insets: fitted V versus [S] and V_{max} versus [I] are shown, [I] is inhibitor.

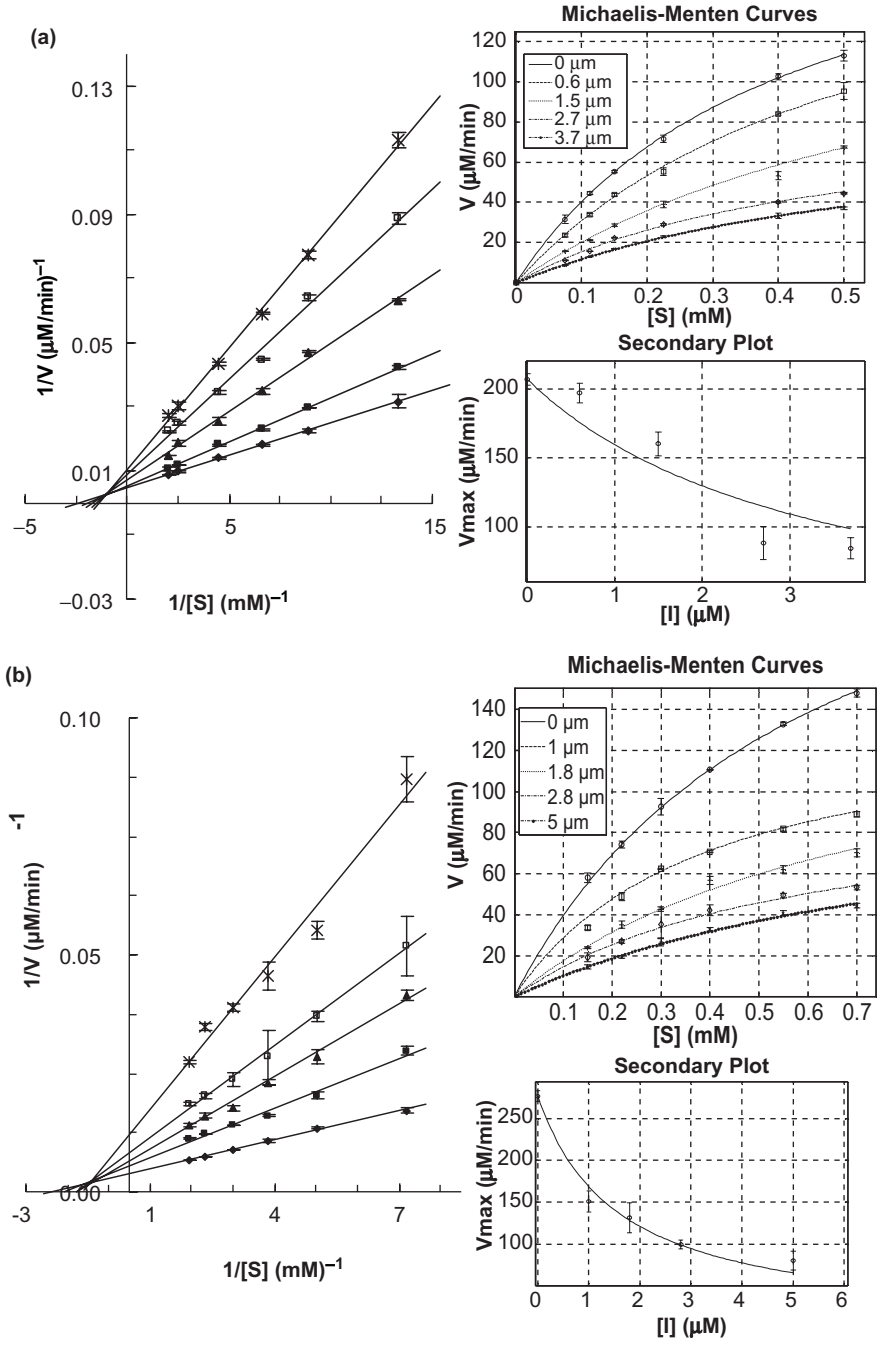

Figure 6. Double reciprocal Lineweaver–Burk plots and nonlinear fittings of MT kinetic assays at temperature of 37°C in the presence of different fixed concentrations of **II** for cresolase reactions (a): 0.0 μM (◆), 0.6 μM (■), 1.5 μM (□), 2.7 μM (▲), 3.7 μM (*), and for catecholase reactions (b): 0.0 μM (◆), 1.0 μM (■), 1.8 μM (□), 2.8 μM (▲), 5.0 μM (*). Insets: fitted V versus [S] and V_{max} versus [I] are shown, [I] is inhibitor.

All thermodynamics parameters were calculated and are summarized in Table 1.

These data suggest that the binding process for the inhibitor is spontaneous at both temperatures ($\Delta G° < 0$). Besides, the binding process of **I** seems to be only entropy driven ($\Delta S° > 0$) in the inhibition of both activities. This is the reason why raising the temperature during catecholase and cresolase inhibition caused a decrease in the K_I value of the inhibitor. Therefore, the interaction between **I** and MT is probably hydrophobic[58]. In addition, there is no interaction between the substrate and inhibitor binding sites in noncompetitive inhibition. Some thiol compounds act as inhibitors of tyrosinase[59] due to their ability to chelate Cu^{2+}. It seems that benzyldithiocarbamate's hydrophobic tail interacts with tyrosinase. Entropy changes in catecholase and cresolase inhibition suggest that activities of tyrosinase develop through hydrophobic interactions[60]. The IC_{50} value of catecholase activity at 0.5 mM of L-DOPA was determined by plotting [S]/V versus inhibitor concentration[56]. It was 9.7 μM (data not shown). Compound **I** is a more potent inhibitor than cinnamic acid, which shows that the sulfur atom plays an important role in inhibitory activity[61].

Table 2. Thermodynamic parameters of binding **II** on mushroom tyrosinase at two different temperatures (±SD).

Reaction type	Temperature (°C)	K_I (μM)	α	K_a ($M^{-1} \times 10^5$)	$\Delta G°$ (kJ.mol^{-1})	$\Delta H°$ (kJ.mol$^{-1)}$	$T\Delta S°$ (kJ.mol^{-1})
Cresolase	27	0.64±0.23	3.8±0.7	15.6±5.6	–35±1	–30±7	–5±2
	37	0.95±0.25	3.5±1.1	10.5±2.8	–36±1		–5±1
Catecholase	27	0.29±0.05	2.8±0.8	34.5±5.9	–37±1	–99±3	–61±4
	37	1.05±0.14	2.3±0.3	9.5±1.2	–35±1		–61±4

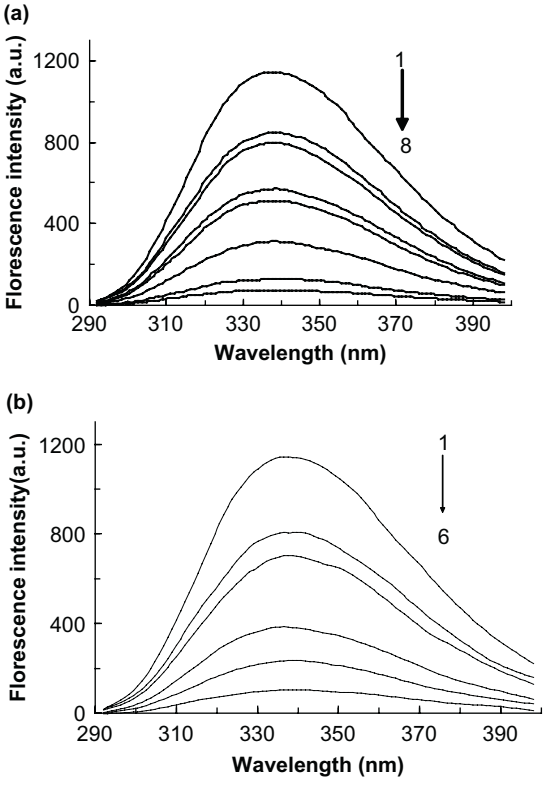

Figure 7. Intrinsic fluorescence emission spectra of MT (1) and MT in the presence of: (a) **I** at concentrations of 1.4 μM (2), 2.5 μM (3), 3.8 μM (4), 4.4 μM (5), 5 μM (6), 10 μM (7), 15 μM (8) and (b) **II** at concentrations of 0.6 μM (2), 1 μM (3), 2 μM (4), 3 μM (5), 5 μM (6). The excitation wavelength was 280 nm. The concentration of the enzyme was 0.17 mg/mL.

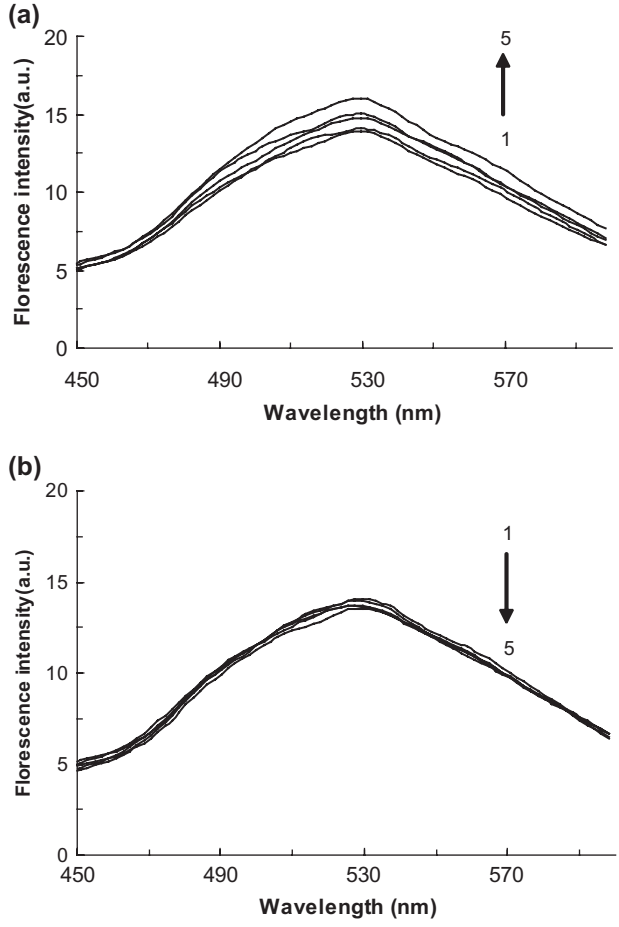

Figure 8. Extrinsic fluorescence emission spectra of ANS-labeled MT in the absence (1) and presence of: (a) **I** at concentrations of 2 μM (2), 5 μM (3), 10 μM (4), 20 μM (5) and (b) **II** at concentrations of 1 μM (2), 2 μM (3), 3 μM (4), 5 μM (5). The excitation wavelength was 385 nm. The concentration ratio (ANS/MT) was 50.

Kinetic parameters of inhibitory effect of p-xylidine-bis(dithiocarbamate) sodium salt on activities of MT

Double reciprocal Lineweaver–Burk plots for the cresolase and catecholase activities of MT on hydroxylation of L-tyrosine and L-DOPA as substrates, in the presence of different fixed concentrations of compound **II** at pH 6.8 and temperatures 27 and 37°C, are shown in Figures 5 and 6. For both activities at both temperatures, **II** behaved as a mixed type inhibitor, since increasing the **II** concentration resulted in a family of lines with a common intercept on the left hand side of the vertical axis and close to the horizontal axis with different slopes, which confirmed mixed inhibition. The equilibrium constant for inhibitor binding with free MT, K_I, was obtained from nonlinear regression fittings as described earlier (shown in the insets of Figures 5 and 6).

At temperature 27°C, the obtained inhibition constants were 0.64 μM for cresolase activity and 0.29 μM for catecholase activity, as summarized in Table 2. In addition, raising the temperature to 37°C caused an increase in inhibition constant values. Obtained constants were 0.95 μM and 1.05 μM for cresolase and catecholase activities, respectively, at 37°C. The inhibition mode of **II** in both activities was mixed type (competitive–noncompetitive) at both temperatures. This indicates that binding of the inhibitor to tyrosinase decreases the strength of binding of the substrate to the active site. This decrease can be assayed with a quantity named α (interaction factor). Experimental data (initial velocities) were fitted in Michaelis–Menten equations in order to obtain apparent maximum velocities (V'_{max}) and K'_m. In mixed type inhibition, V'_{max} decreases by a factor $(1 + [I]/\alpha K_I)$. So, α and K_I can be obtained from the fitting of V'_{max} versus $[I]$, as summarized in Table 2. In order to understand the effect of temperature on inhibition, the changes of Gibbs standard free energy, entropy,

and enthalpy of binding were calculated using the association binding constant (K_a) and are summarized in Table 2. Negative enthalpy changes indicate that a strong attachment of compound **II** develops through electrostatic forces. Also, the IC_{50} value of catecholase activity at 0.5 mM of L-DOPA was 0.7 μM (data not shown).

Florescence studies

The conformational change of MT after the binding of compounds **I** and **II** was investigated by fluorescence emission spectroscopy of inhibited MT. Changes in the fluorescence emission spectra of tyrosinase (intrinsic protein fluorescence) after incubation with increasing concentrations of inhibitors are shown in Figure 7. Increasing inhibitor concentration caused the fluorescence emission intensity to decrease, without a shift of the emission maximum. In order to better consider tertiary structure changes of the protein we labeled MT with ANS as an extrinsic fluorophore. The added inhibitors did not change the extrinsic emission considerably. Figure 8 shows little structural change. On the other hand, the absorbance spectra of the inhibitors did not show considerable absorbance at the intrinsic emission area of MT (data not shown). So, the conformation of inhibitor-bound MT was stable and more rigid than that of uninhibited MT[62].

In recent studies, we have considered the inhibitory effects of some thiol compounds such as *n*-alkyl dithiocarbamates, *n*-alkyl xanthates, and benzylthiol[48,49,60]. It is apparent that thiols are chelating groups of the MT active site[63]. Furthermore, it is evident that the aromatic ring as an electron-withdrawing group can increase inhibitory effects[64,65]. Results of our analysis show that inhibition constants for cresolase and catecholase activity inhibition of MT are approximately equal. Thus, it seems that compound **I** interacts with the hydrophobic pocket of the active site due to the hydrophobic tail, without any substrate interactions. Therefore, benzyldithiocarbamate behaves as a noncompetitive inhibitor. Probably compound **II**, due to two charged groups, will decrease the affinity of substrates to the active site. IC_{50} values show that the bifunctional inhibitor is more potent than the monofunctional inhibitor. It seems that two ionic negatively charged heads can chelate positively charged copper ions.

Acknowledgements

The financial support given by the University of Tehran is gratefully acknowledged.

References

1. Yoruk R, Marshall MR. Physicochemical properties and function of plant polyphenol oxidase: a review. J Food Biochem 2003; 27:361–422.
2. Seo SY, Sharma VK, Sharma N. Mushroom tyrosinase: recent prospects. J Agric Food Chem 2003;51:2837–53.
3. Van Gelder CWG, Flurkey WH, Wichers HJ. Sequence and structural features of plant and fungal tyrosinases. Phytochemistry 1997;45:1309–23.
4. Halaouli S, Asther M, Sigoillot J-C, Hamdi M, Lomascolo A. Fungal tyrosinases: new prospects in molecular characteristics, bioengineering and biotechnological applications. J Appl Microbiol 2006;100:219–32.
5. Mayer AM. Polyphenol oxidases in plants and fungi: going places? A review. Phytochemistry 2006;67:2318–31.
6. Robb DA. Copper Proteins and Copper Enzymes. Boca Raton: CRC Press, 1984.
7. Riley PA. Tyrosinase kinetics: a semi-quantitative model of the mechanism of oxidation of monohydric and dihydric phenolic substrates. J Theor Biol 2000;203:1–12.
8. Fenoll LG, Rodriguez-Lopez JN, Garcia-Sevilla F, Tudela J, Garcia-Ruiz PA, Varon R. Oxidation by mushroom tyrosinase of monophenols generating slightly unstable oquinones. Eur J Biochem 2000;267:5865–78.
9. Nylander K, Bourdon J-C, Bray SE, Gibbs NK, Kay R, Hart I, et al. Transcriptional activation of tyrosinase and TRP-1 by p53 links UV irradiation to the protective tanning response. J Pathol 2000;190:39–46.
10. Jaenicke E, Decker H. Tyrosinases from crustaceans form hexamers. Biochem J 2003;371:515–23.
11. Jacobson ES. Pathogenic roles for fungal melanins. Clin Microbiol Rev 2000;13:708–17.
12. Barrett FM. Wound-healing phenoloxidase in larval cuticle of Calpodes ethulius (Lepidoptera: Hesperiidae). Can J Zool 1984;62:834–8.
13. Sugumaran M. Molecular mechanism for culticular sclerotization. Adv Insect Physiol 1988;21:179–231.
14. Sugumaran M. Molecular mechanisms for mammalian melanogenesis. Comparison with insect cuticular sclerotization. FEBS Lett 1991;295: 233–9.
15. Goding CR. Melanocytes: the new black. Int J Biochem Cell Biol 2007;39:275–9.
16. Spritz RA. The genetics of generalized vitiligo and associated autoimmune diseases. J Dermatol Sci 2006;41:3–10.
17. Strothkemp KG, Jolley RL, Mason HS. Quaternary structure of mushroom tyrosinase. Biochem Biophys Res Commun 1976;70:519–24.
18. Decker H, Schweikardt T, Tuczek F. The first crystal structure of tyrosinase: all questions answered?Angew Chem Int Ed Engl 2006;45:4546–50.
19. Sanchez-Ferrer A, RodriGuez-Lopez JN, Garcia-Canovas F, Garcia-Carmona F. Tyrosinase: a comprehensive review of its mechanism. Biochim Biophys Acta 1995;1247:1–11.
20. Fenoll LG, Rodriguez-Lopez JN, Garcia-Sevilla F, Garcia-Ruiz PA, Varo NR, Garcia-Canovas F, et al. Analysis and interpretation of the action mechanism of mushroom tyrosinase on monophenols and diphenols generating highly unstable *o*-quinone. Biochim Biophys Acta 2001;1548:1–22.
21. Rajarathnam S, Shashirekha MN, Rashmi S. Biochemical changes associated with mushroom browning in Agaricus bisporus (Lange) Imbach and Pleurotus florida (Block and Tsao): commercial implications. J Sci Food Agric 2003;83:1531–7.
22. Friedman M. Food browning and its prevention: an overview. J Agric Food Chem 1996;44:631–53.
23. Rescigno A, Sollai F, Pisu B, Rinaldi A, Sanjust E. Tyrosinase inhibition: general and applied aspects. J Enzyme Inhib Med Chem 2002;17:207–18.
24. Kenji O, Minako K, Yoshihide S, Seiichi K, Yuki M, Yoshinori N, et al. Inhibitory effects of whisky congeners on melanogenesis in mouse B16 melanoma cells. Biosci Biotech Biochem 2008;72:1107–10.
25. Palumbo A, Ischia M, Misuraca G, Prota G. Mechanism of inhibition of melanogenesis by hydroquinone. Biochim Biophys Acta 1991;1073: 85–90.
26. Maeda K, Fukuda M. In vitro effectiveness of several whitening cosmetic components in human melanocytes. J Soc Cosmet Chem 1991;42: 361–8.
27. Riely PA, Sawyer B, Wolff MA. The melanocytotoxic effect of *4*-hydroxyanisole. J Invest Dermatol 1975;64:86–9.
28. Kim Y-J, Uyama H. Tyrosinase inhibitors from natural and synthetic sources: structure, inhibition mechanism and perspective for the future. Cell Mol Life Sci 2005;62:1707–23.
29. Naish S, Holden JL, Cooksey CJ, Riely PA. The major primary cytotoxic product of *4*-hydroxyanisole oxidation by mushroom tyrosinase is *4*-methoxy ortho benzoquinone. Pigment Cell Res 1988;1:382–5.
30. Riely PA. Melanogenesis: a realistic target for antimelanoma therapy. Eur J Cancer 1991;27:1172–7.
31. Badria FA, Gayyar MA. A new type of tyrosinase inhibitors from natural products as potential treatments for hyperpigmentation. Boll Chim Farma 2001;140:267–71.

32. Kubo I, Kinst-Hori I. Tyrosinase inhibitors from anise oil. J Agric Food Chem 1998;46:1268–71.
33. Kubo I, Kinst-Hori I. Tyrosinase inhibitors from cumin. J Agric Food Chem 1998;46:5338–41.
34. Kubo I, Kinst-Hori I. Tyrosinase inhibitory activity of the olive oil flavor compounds. J Agric Food Chem 1999;47:4574–8.
35. Kubo I, Kinst-Hori I. *2*-Hydroxy-*4*-methoxy benzaldehyde: a potent tyrosinase inhibitor from African medicinal plants. Planta Med 1999;65:19–22.
36. Jimenez M, Chazarra S, Escribano J, Cabanes J, Garcia-Carmona F. Competitive inhibition of mushroom tyrosinase by 4-substituted benzaldehydes. J Agric Food Chem 2001;49:4060–3.
37. Espin JC, Wichers HG. Effect of captopril on mushroom tyrosinase activity in vivo. Biochim Biophys Acta 2001;1554:289–300.
38. Andrawis A, Khan V. Effect of methimazole on the activity of mushroom tyrosinase. Biochem J 1996;35:91–6.
39. Ferrar PH, Walker JRI. Inhibition of diphenoloxidases: a comparative study. J Food Biochem 1996;20:15–30.
40. Lee KH, Koketsu M, Choi SY, Lee KJ, Lee P, Ishihara H, et al. Potent inhibitory effects of N-aryl S-alkylthiocarbamate derivatives on the dopa oxidase activity of mushroom tyrosinase. Chem Pharm Bull 2005;53:747–9.
41. Seiji M, Yashida T, Itakura H, Irimajiri T. Inhibition of melanin formation by sulfhydryl compounds. J Invest Dermatol 1969;52:280–6.
42. Kasraee B, Hügin A, Tran C, Sorg O, Saurat J-H. Methimazole is an inhibitor of melanin synthesis in cultured B16 melanocytes. J Invest Dermatol 2004;122:1338–41.
43. Anderson JW. Extraction of enzyme and sub cellular organelles from plant tissues. Phytochemistry 1968;7:1973–88.
44. Palmer JK, Robbert JB. Inhibition of banana polyphenol oxidase by 2-mercaptobenzothiazole. Science 1967;157:200–1.
45. Ronconi L, Maccato C, Barreca D, Saini R, Zancato M, Fregona D. Gold (III) dithiocarbamate derivatives of N-methylglycine: an experimental and theoretical investigation. Polyhedron 2005;24:521–31.
46. Faraglia G, Sitran S, Montagner D. Pyrrolidine dithiocarbamates of Pd (II). Inorg Chim Acta 2005;358:971–80.
47. Kim I, Kim CH, Kim JH, Lee J, Choi JJ, Chen ZA, et al. Pyrrolidine dithiocarbamate and zinc inhibit proteasome-dependent proteolysis. Exp Cell Res 2004;298:229–38.
48. Gheibi N, Saboury AA, Mansury-Torshizy H, Haghbeen K, Moosavi-Movahedi AA. The inhibition effect of some n-alkyl dithiocarbamates on mushroom tyrosinase. J Enzyme Inhib Med Chem 2004;20:393–9.
49. Alijanianzadeh M, Saboury AA, Mansouri-Torshizi H, Haghbeen K, Moosavi-Movahedi AA. The inhibitory effect of some new synthesized xanthates on mushroom tyrosinase activities. J Enzyme Inhib Med Chem 2007;22:239–46.
50. Mansouri-Torshizi H, Islami-Moghaddam M, Divsalar A, Saboury AA. 2,2′-Bipyridinebutyldithiocarbamatoplatinum (II) and palladium (II) complexes: synthesis, characterization, cytotoxicity, and rich DNA-binding studies. Bioorg Med Chem 2008;16:9616–25.
51. Cabanes J, Garcia-Canovas F, Lozano JA, Garcia-Carmona F. A kinetic study of the melanization pathway between L-tyrosine and dopachrome. Biochim Biophys Acta 1987;790:101–7.
52. Chen QX, Kubo I. Kinetics of mushroom tyrosinase inhibition by quercetin. J Agric Food Chem 2002;50:4108–12.
53. Marangoni AG. Enzyme Kinetics: A Modern Approach. New York: John Wiley & Sons, 2002.
54. Tellinghuisen J. Stupid statistics! Methods Cell Biol 2008;84:739–80.
55. Tellinghuisen J. Least squares in calibration: weights, nonlinearity, and other nuisances. Methods Enzymol 2009;454:259–85.
56. Cortes A, Cascante M, Cardenas M, Cornish-Bowden A. Relationships between inhibition constants, inhibitor concentrations for 50% inhibition and types of inhibition: new ways of analyzing data. Biochem J 2001;357:263–8.
57. Atkins P, DePaula J. Physical Chemistry, 7th ed. New York: WH Freeman & Company, 2002: Ch. 9.
58. Perozzo R, Folkers G, Scapozza L. Thermodynamics of protein–ligand interactions: history, presence, and future aspects. J Recept Signal Transduct Res 2004;24:1–52.
59. Hanlon DP, Shuman S. Copper ion binding and enzyme inhibitory properties of the anti thyroid drug methimazole. Experientia 1975;31:1005–6.
60. Saboury AA, Zolghadri S, Haghbeen K, Moosavi-Movahedi AA. The inhibitory effect of benzenethiol on the cresolase and catecholase activities of mushroom tyrosinase. J Enzyme Inhib Med Chem 2006;21:711–17.
61. Shi Y, Chen QX, Wang Q, Song KK, Qiu L. Inhibitory effects of cinnamic acid and its derivatives on the diphenolase activity of mushroom (*Agaricus bisporus*) tyrosinase. Food Chem 2005; 92:707–12.
62. Park KH, Lee JR, Hahn HS, Kim YH, Bae CD, Yang JM, et al. Inhibitory effect of ammonium tetrathiotungstate on tyrosinase and its kinetic mechanism. Chem Pharm Bull 2006;54:1266–70.
63. Liu J, Yi W, Wan Y, Ma L, Song H. 1-(1-Arylethylidene)thiosemicarbazide derivatives: a new class of tyrosinase inhibitors. Bioorg Med Chem 2008;16:1096–102.
64. Karbassi F, Saboury AA, Hassan Khan MT, Iqbal Choudhary M, Saifi ZS. Mushroom tyrosinase inhibition by two potent uncompetitive inhibitors. J Enzyme Inhib Med Chem 2004;19:349–53.
65. Liu J, Cao R, Yi W, Ma C, Wan Y, Zhou B, et al. A class of potent tyrosinase inhibitors: alkylidenethiosemicarbazide compounds. Eur J Med Chem 2009;44:1773–8.